Desalination 444 (2018) 44–52

Contents lists available at ScienceDirect

Desalination

journal homepage: www.elsevier.com/locate/desal

A hybrid reverse osmosis/adsorption desalination plant for irrigation and drinking water

M. Sarai Atab[a,b], A.J. Smallbone[a,*], A.P. Roskilly[a]

[a] Sir Joseph Swan Centre for Energy Research, Newcastle University, Newcastle Upon Tyne NE1 8ST, UK
[b] The University of Wasit, Wasit, Iraq

ARTICLE INFO

Keywords:
Desalination
Adsorption
Hybridisation
Reverse Osmosis

ABSTRACT

The hybridisation of brackish water reverse osmosis (BWRO) desalination technology and an adsorption cycle (AD) are considered in this work as a means of producing large quantities of a) water for irrigation and; b) high quality water for domestic use. The RO process and the AD cycle are represented as numerical models and have been optimised to produce fresh water and cooling. An existing RO plant can be retrofitted to become an RO-AD process to improve its specific energy consumption and simultaneously produce a cooling effect which can be exploited for local process cooling or air conditioning. A pressure exchanger (PX) and AD are combined to recover the reject from the RO, resulting in reduction in power consumption. The hybridised RO-AD desalination processes can be considered as the optimum solution for rural areas due to its capability for the production of water for irrigation and drinking as well as cooling for air-conditioning. Nevertheless, the temperature and feed salinity may negatively effect on RO production, with the AD cycle producing more than 6 m^3/tonne s.g of drinking water (< 15 ppm) at 85 °C, additionally the AD evaporator is not effected significantly by salinity. The proposed plant could produce 24,000 m^3/day for irrigation and 6.3 m^3/tonne s.g for drinking as well as 75 RTon/tonne s.g. Another interesting finding was that the minimum specific energy for the combined RO-PX-AD plant with a capacity of 24,000 m^3/day is 0.8 kWh/m^3 at RO recovery = 45%. The small-scale combined system was also examined to produce 2000 m^3/day and cost of different configurations was estimated as well. The results showed that the cost of the combined RO-AD system is the lowest, 0.44 £/m^3 compares with other RO configurations.

1. Introduction

Despite three quarters of the earth surface being covered by water, 97.5% of the water on the earth surface is seawater with TDS higher than 35,000 ppm. In the 2.5% of the total fresh water, only 30% is suitable for use because the majority of 69% fresh water is frozen in the icecaps and glaciers [1]. Around 71% of the total global fresh water withdrawal (3100 billion m^3) is used for agriculture purposes and by 2030, if there are no efficiency gains, it will increase to 4500 billion m^3 [2,3]. The gap between demand and supply can be filled by several types of desalination processes. Desalination is a significant method for producing potable water for human drinking, irrigation and industry [4,5]. There are numerous well established desalination technologies which have been developed commercially aimed to reduce power consumption, shown in Table 2. The best and most practical desalination plants offer a cost-effective solution for removing suspended salt or solid from sea or brackish water to produce potable water while being environmentally friendly. Among existing desalination plants, the Reverse Osmosis (RO) and Multi-Stage Flash (MSF) technologies represent 66% and 21% respectively of all these plants producing 77.4 million m^3 per day [1]. However, energy consumption for all types of desalination technologies remains high.

The number of Reverse Osmosis (RO) processes in major desalination plants have expanded considerably in recent times [6]. In an RO purification system, a semi-permeable membrane removes ions, proteins, and organic chemicals, often not easily accomplished with conventional methods [7]. An RO system's advantages include a small land footprint, a modular design and the availability of automatic process control and comparatively low-cost water production [8]. RO desalination plants have been frequently called into service for water and wastewater treatment, particularly in those areas where water is scarce [9]. Also, the RO process is recommended by Al-Karaghouli and Kazmerski [10] to address a brackish water, and is considered more cost effective economically when TDS is > 5000 ppm. Nevertheless, RO

* Corresponding author.
E-mail address: andrew.smallbone@newcastle.ac.uk (A.J. Smallbone).

https://doi.org/10.1016/j.desal.2018.07.008
Received 15 December 2017; Received in revised form 30 May 2018; Accepted 8 July 2018

Nomenclature

J_W	Permeate flux, m/s
A_w	Permeability coefficient m/s-Pa
ΔP	Pressure difference, Pa
D_w	Water diffusivity, m^2/s
C_w	Water concentration, mol/m^3
V_w	Water molar volume, m^3
J_s	Solute transport, m/s
B_s	Solute transport parameter, m/s
Cm	Solute concentration in the membrane, mol/m^3
Cp	Solute concentration at permeate, mol/m^3
Bs	Solute transport parameter, m/s
Ds	Diffusivity of solute, m/s
Ks	Solubility of solute, m^2/s
Rs	Salt rejection, %
Pf	Feed water pressure, Pa
Qf	Feed flow rate, m^3/day
E	Specific energy consumption, kWh/m^3
$\Delta\pi$	Osmotic pressure difference, Pa
Qr	Rejected flow rate, m^3/day
Qp	Permeate flow rate, m^3/day
Pp	Permeate pressure, Pa
Cf	Concentration of feed water, mol/m^3
q	Uptake by adsorbent material, kg kg^1
Q	Total heat or energy, W
*q**	Equilibrium uptake, kg kg^{-1}
$\dot{m}$	Mass flow rate, kg s^{-1}
M_a	Mass, kg
t	Time, sec
hfg	Latent heat, kJ kg^{-1}
t-cycle	Number of cycles per day
k	Thermal conductivity, W m^{-1} k^{-1}
T	Temperature, K
E	Specific energy consumption, kWh/m^3
E_{pump}	Pump energy consumption, kWh
A	Area, m^2
Cr	Concentration in the concentrate, mol/m^3

Subscripts

f	Feed water
p	Permeate
r	Rejected
ads	Adsorption
des	Desorption
HX	Heat exchanger
out	Outlet
hw	Hot water
cw	Cooling water
cond	Condenser
evap	Evaporator
sg	Silica gel
b	Brine

Greek symbols

η	Efficiency, %
δm	Membrane thickness, m

Abbreviations

ERD	Energy recovery device
RO	Reverse osmosis
HPP	High pressure pump
BWRO	Brackish water
PX	Pressure exchanger
SCP	Specific cooling power

desalination technologies have shortcomings such as high energy requirement, high maintenance and high amount of rejected water [6,7,11].

The RO process performance is strongly influenced by feed water temperature due to the impact of a reduction in solution viscosity [12,13] and expansion of membrane pores which finally results in an increase of permeate production [14]. Jin et al. have studied the effects of feed water temperature on separation performance for brackish water RO membranes [15]. A range of feed water temperatures (15, 25, and 35 °C) were used to treat brackish water by RO membranes. Model

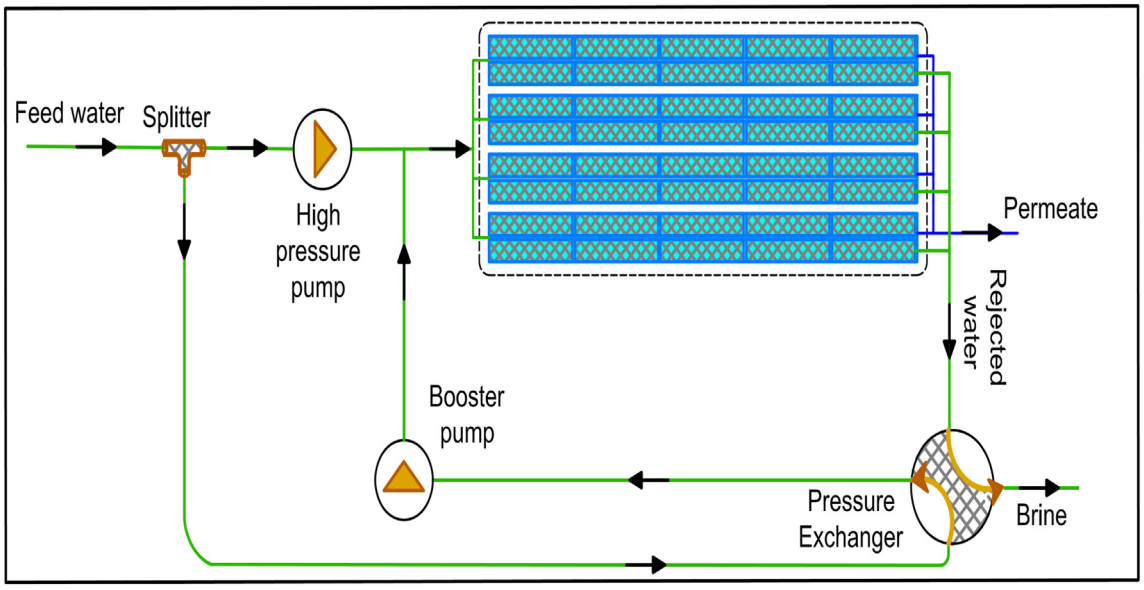

Fig. 1. Schematic diagram of the RO plant.

Table 1
The RO model conditions.

	TDS, kg/kg	Temperature, °C	Pressure, bar	Flow rate, m^3/h
Feed	0.015	25	30	2224
Product	0.0003	25	2	1000
Reject	0.027	25	28	1224

results and experimental data confirmed that solute concentration polarization decreases, while water permeability and salt permeability increased with temperature. Their results also demonstrated that the rate of energy consumption decreases with higher feed water temperature. These results agree with Jawor and Hoek [16] who concluded that the high temperature operation of brackish water RO processes could enable higher recovery and lower energy consumption.

In recent years, those more conventional technologies have been overtaken by adsorption desalination technology in terms of the production of high-grade fresh potable water with salinity levels as low as 10 ppm, reduced electricity consumption (only 1.38 kWh/m^3) and CO_2 emissions of 0.6 kg/m^3, accompanied by a reduced water production cost of 0.16 £/m^3 [11]. It is a novel and promising technology that is attracting more research [11,17–27].

Three main components comprise the adsorption water desalination cycle: 1) the adsorption/desorption bed, 2) the evaporator and, 3) condenser producing desalinated water (from the condenser) and cooling (from the evaporator) [28,29]. The evaporator receives sea or brackish water which is evaporated by means of adsorption. Heat is extracted from the chilled water passing through the evaporator coil, thus yielding a cooling effect [29]. During the adsorption, the adsorbent material adsorbs water vapour while in the desorption process, the water vapour is regenerated by heating, followed by condensation in the condenser where the fresh water product is obtained [30].

By using a combination of the MSF (multi-stage flash) and RO, Helal et al. [31] explored the feasibility of the hybridisation of the processes and thereby the potential of reducing the MSF process costs by between 17% and 24%. A hybrid of Adsorption Desalination with MED (Multi Effect Distillation) (ADMED) has been conducted to perform better than the above [22,32], with more than twice as much water being produced, in comparison with the conventional MED plant. It also contributed to cooling which, as stated above, can in-principle be used for process cooling or air conditioning. Thu et al. investigated the performance of 4-bed adsorption desalination cycle [26] while Mitra et al. have reported a single and two stage modes [33]. Systems for the production of potable water and cooling power have been developed by Saha et al., utilising 3-bed and two evaporators [34]. The internal heat in the condenser has been used for multiple evaporation in advanced cycle. Thu et al., developed a multi-effect adsorption desalination (MEAD) to recover energy from the condensation heat to improve water production at low temperatures below 35 °C [35].

This paper deals with the combination between RO and AD, feeding the reject from BWRO to the AD evaporator, thus producing water in large quantities and of high quality both for irrigation and drinking. In addition, the system provides cooling for an air conditioning demand. Most significantly for the purposes of this study, it has been used to treat brackish water by utilising the combined RO-AD system. Also, this work studies the effect of various factors including, temperature, pressure and an energy recovery device (PX) by developing a numerical code. Moreover, the optimum operating conditions were explored to minimize specific energy consumption and maximize water production for multi-purposes. Furthermore, this work examines a large-scale RO-

Table 3
Numerical model equations describing the RO desalination process.

Model parameter and definition		Equation no.	Reference no.
Solvent transport	$J_W = A_w(\Delta P - \Delta\pi)$	1	[40–43]
Solvent permeability	$A_W = \frac{D_W C_W V_W}{\delta_m RT}$	2	[40,43,44]
Solute transport	$J_s = B_s(C_m - C_p)$	3	[41–43,45]
Solute permeability	$B_s = \frac{D_S K_S}{\delta_m}$	4	[43,44]
Salt rejection	$R = \left[1 + \frac{B}{A(\Delta\rho - \Delta\pi)}\right]^{-1}$	5	[43]
Osmotic pressure	$\Delta\pi = RT\Sigma(n/v)$	6	[41,44]
Specific energy	$E = \frac{P_f Q_f (\varepsilon_{pump})^{-1} - P_r Q_r \varepsilon_{ERD}}{Q_p}$	7	–
Total mass balance	$Q_f C_f = Q_p C_p + Q_r C_r$	8	–

Table 4
Dubinin-Astakhov equation co-efficients.

Symbol	Value	Unit
q_0	0.46826	kg/kg of adsorbent
E	10.0887	kJ/mol
n	5.6476	(−)
R	8314	J/mol·K

Table 5
Model validation for AD cycle against reported measurement data.

Hot temperature (°C)	SDWP (simulation) (m^3/day)	SDWP (experiment) (m^3/day)	Error %
65	5.31	5.64	−6.21
70	6.1	6.19	−1.48
75	6.9	7.31	−5.94
80	7.5	8.08	−7.73
85	8.2	8.59	−4.76

Table 6
The AD model conditions.

	TDS, kg/kg	Temperature, °C
Feed	0.027	T_{hw} = 85
Product	< 0.00001	T_{cw} = 29.8
		$T_{chilled}$ = 30

Table 2
Comparison of different desalination processes [5,10,11,24].

Properties	MSF	MED	MVC	TVC	SWRO	BWRO	ED	AD
Operation temperature	35–120	35–100	30–60	> 120	20–40	20–40	20–40	55–85
Pre-treatment requirement	Low	Low	Low	Low	High	High	High	Low
Typical unit size (m^3/day)	50,000–70,000	5000–15,000	100–3000	10,000–30,000	Up to 128,000	Up to 98,000	2–145,000	(25)[b]
Electrical energy consumption (kWh/m^3)	2.5–5	2–2.5	7–12	1.8–1.6	(4–6) [a]	1.5–2.5	2.64–5.5	Less than 1.5
thermal energy consumption (kWh/m^3)	15.83–23.5	12.2–19.1	None	14.5	None	None	None	Energy from waste heat
Total electricity consumption (kWh/m^3)	18.33–28.5	14.2–24.1	7–12	16.26	4–6	1.5–2.5	2.64–5.5	5.63
Product water quality (ppm)	≈10	≈10	≈10	≈10	400–500	200–500	150–500	< 10

[a] Including recovery system energy.
[b] Including internal heat recover.

Table 7
Mathematical model equations for the AD cycle [49–51].

Parameter	Mathematical equation	Equation no.
Uptake of water vapour	$q^* = q_0 \exp\left[-\left(-\frac{RT}{E}\ln\left(\frac{P}{P_0}\right)\right)^n\right]$	9
Kinetic of adsorption or desorption	$\frac{dq(t)}{dt} = K(q^* - q(t))$	10
Thermal conductivity	$K = \frac{15\,D_{sor}e^{\frac{E_a}{RT}}}{R_p^2}$	11
Mass balance of the cycle	$\frac{dM_{s,evap}}{dt} = \dot{m}_{s,in} - \dot{m}_{d,cond} - \dot{m}_b$	12
Heat of evaporation	$Q_{evap} = \dot{m}_{chilled} c_p (T_{chilled})(T_{chilled,in} - T_{chilled,out})$	13
Condensation energy	$Q_{cond} = \dot{m}_{cond} c_p (T_{cond})(T_{cond,out} - T_{cond,in})$	14
Evaporator energy balance	$[M_{s,evap} c_{p,s} (T_{evap} X_{s,evap}) + M_{HX} c_{p,HX}]\frac{dT_{evap}}{dt} = \theta \times h_f (T_{evap}, X_{s,evap})\dot{m}_{s,in} - n \times h_{fg}(T_{evap})\left[A\left(\frac{dq_{ads}}{dt}\right) + B\left(\frac{dq_{ads}}{dt}\right)\right] + \dot{m}_{chilled} c_p (T_{evap})(T_{chilled,in} - T_{chilled,out}) - \gamma h_f (T_{evap}, X_{s,evap})\dot{m}_{brine}$	15
Adsorption/desorption bed energy balance	$[M_a c_{(p,a)} + M_{HX} c_{p,HX} + + M_{abe} c_{p,abe}]\frac{dT_{ads/des}}{dt} = \pm \dot{m}_{cw/hw} C_p (T'_{cw/hw,in} - T_{cw/hw,out}) \pm z \cdot Q_{st} M_a \frac{dW_{ads/des}}{dt}$	16
Condenser energy balance	$[M_{cond} c_p (T_{cond}) + M_{(HX,cond)} c_{p,HX}]\frac{dT_{cond}}{dt} = h_f \frac{dM_d}{dt} + h_{fg}(T_{cond}) M_a \left(n \cdot \frac{dq_{des}}{dt}\right) + \dot{m}_{cond} C_p (T_{cond}) \times (T_{cond,in} - T_{cond,out})$	17
Specific cooling power	$\mathrm{SCP} = \int_0^{t_{cycle}} \frac{Q_{evap} t}{M_a} \mathrm{dt}$	18
Specific daily production	$SDWP = \int_0^{t_{cycle}} \frac{Q_{cond} t}{h_{fg}(T_{cond}) M_{Sg}} dt$	19

Table 8
The inlet and outlet water temperatures of each indicated stream in (Fig. 2).

Stream number	Temperature (°C)
1	25
2	15
3	30
4	21
5	29.8
6	44.2
7	85
8	41.7
9	29.8
10	31.7
11	29.8
12	15.1
13	30
14	60.7
15	28.6

AD combined system which produces 24,000 m^3/day for irrigation and 6.3 m^3/tonne s.g for drinking as well as 75 RTon/tonne s.g of cooling, and a small-scale RO system producing 2000 m^3/day of fresh water is considered as well in terms of the cost of production.

2. Model development

2.1. A numerical model for RO system

The RO system is a process of separation of water from a salt solution by semi-permeable membranes. Freshwater passes to water compartment as a permeate water with a pressure in excess of the osmotic pressure [7]. A numerical model was established were used to design an RO, the schematic diagram of RO desalination unit incorporated with a pressure exchanger is shown in Fig. 1. The RO system has the following significant components: a pump unit that supplies high feed pressure (*Pf*) and flow rate (*Qf*) to a membrane, RO unit is a group of RO vessels comprised of membrane modules, and energy recovery device such as pressure exchanger that produces energy from rejected stream directly to a pump. To predict RO performance and optimize permeate quality and flow rate, some assumptions were applied in the modelling, such as:

- the solution-diffusion model is valid for the transport of water and solute through the RO membrane;
- the efficiency of the pump and turbine are fixed at 84% and 70% respectively;
- The pressure drop in feed stream is taken as the dead state 101.3 kPa;
- the salt feed water stream is considered to be a dilute solution and is treated as an ideal solution;
- the concentration polarization effect is negligible; [36–38]

The RO model was constructed by utilising the RO equations in Table 3 and validated extensively in previous work [39] and the model conditions is shown in Table 1.

2.2. The adsorption system

Adsorption isotherms and kinetics are the two essential parameters necessary for predicting adsorbent material performance. 'Adsorption isotherms' are the maximum amount of adsorbate that can be adsorbed per unit mass of dry material at a certain pressure ratio. The equations presented in Table 7 (with the co-efficient presented in Table 4 [46]) are the 'Adsorption kinetics', *i.e.* the rate of adsorption or desorption at the operating pressure ratio. Silica gel type-RD was used as the

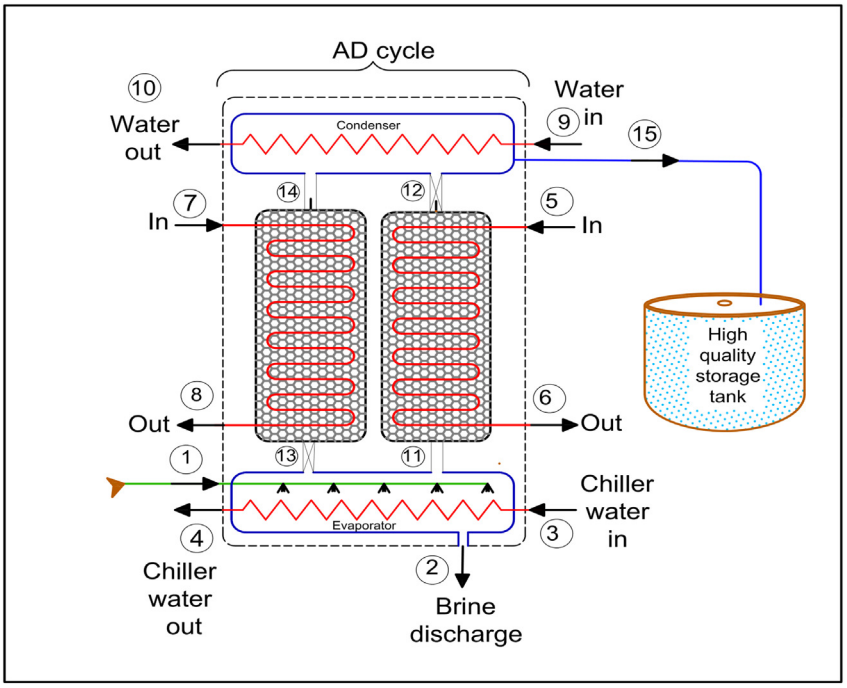

Fig. 2. Schematic of a two-bed adsorption cycle.

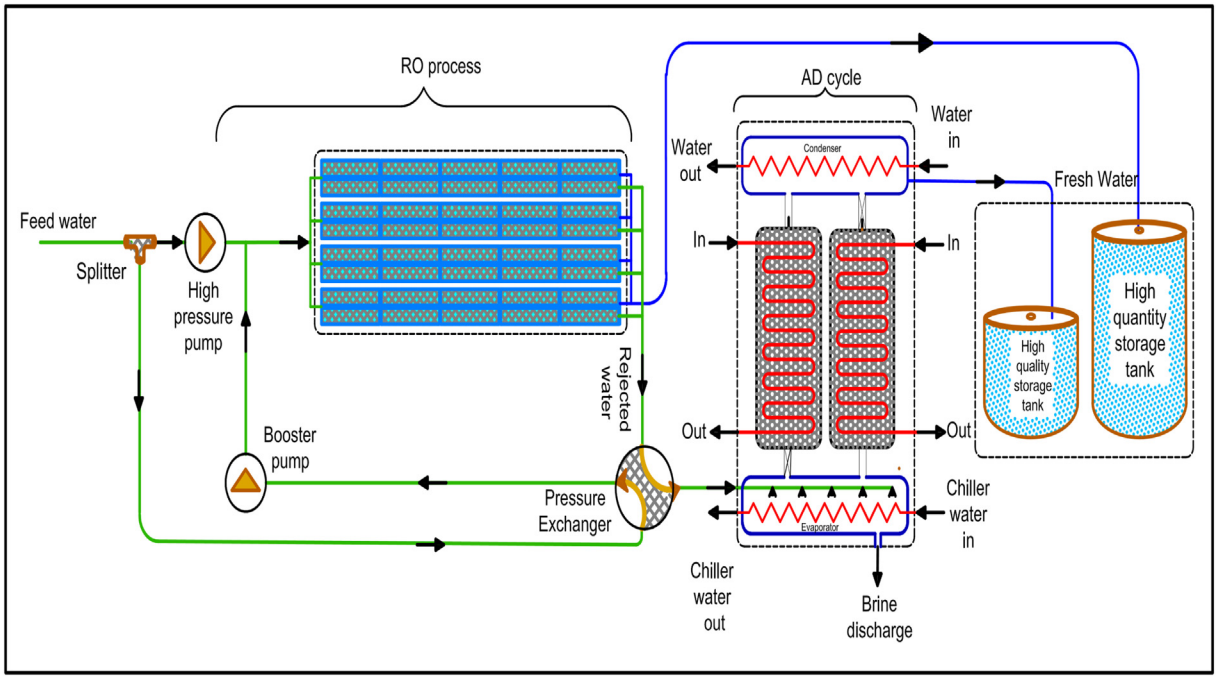

Fig. 3. A schematic diagram presenting the hybrid RO-AD process.

adsorbent, based on the adsorption isotherms, kinetics and energy balances between the sorption elements. The pressure ratio is defined as the ratio between evaporator to bed pressures during the adsorption process or the ratio between condenser to bed pressure during the desorption process [47].

The mathematical models of the AD cycles for the two-bed modes were developed for the production of water and generation of cooling [48]. Fig. 2 shows a schematic diagram of an AD cycle. Three main components make up a typical AD plant: (1) the evaporator; (2) single to multi-reactor beds where the adsorbent (silica gel) is placed, and (3) the condenser. The evaporator takes sea or brackish water discontinuously by means of a pump and evaporation occurs when silica gel takes up the water vapour. The efficiency of the evaporation increases by utilising a spray system. An external heating water supplies to the evaporator to maintain the evaporation process. The rejected brine is discharged intermittently from the evaporator. Unsaturated silica gel is packed into two beds to adsorb the water vapour from the evaporator. By using a process known as desorption, the regenerated water vapour flows to the condenser as distilled water. To simplify the models, the following lumped parameter assumptions are:

- The temperature is uniform throughout the adsorbent (silica gel)

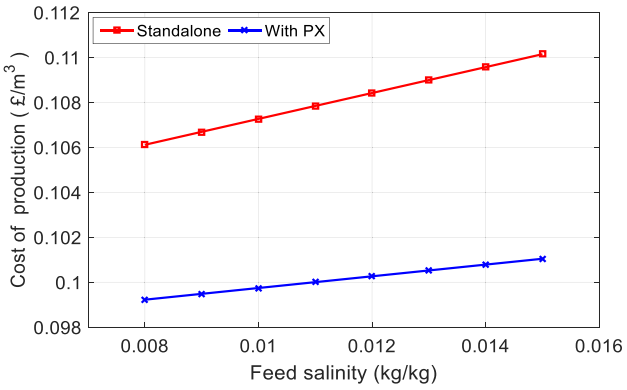

Fig. 4. Cost of RO production as a function of feed salinity.

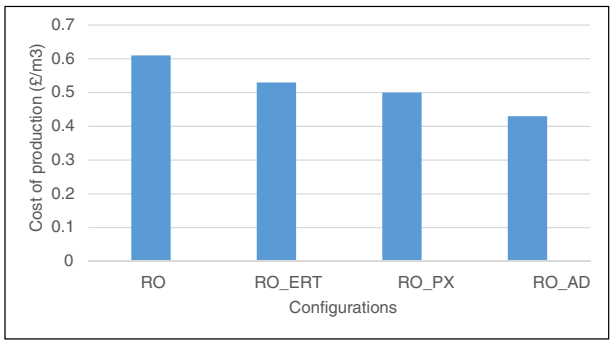

Fig. 6. Cost of production for different RO configurations.

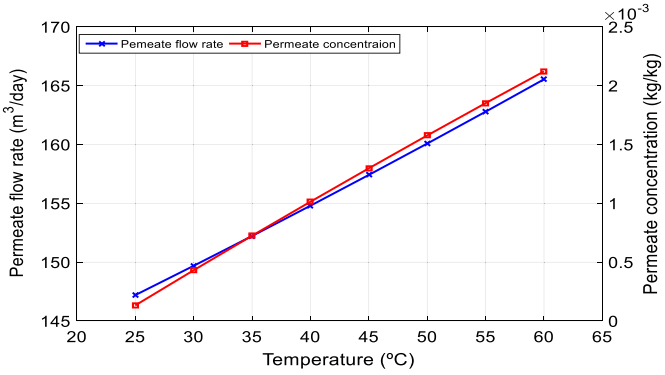

Fig. 7. Effect of temperature on permeate concentration and low rate.

layer;

- The adsorption of the water vapour by the silica gel inside the adsorber bed is uniform;
- Both the adsorbent (silica gel) and the adsorbate gas phases are in a condition of equilibrium.

Detailed thermodynamic models which represent AD cycle have been developed using a numerical code. The models have been validated and calibrated using reported measurement data, and the performance of these technologies have been simulated. The inlet and outlet water temperatures of each indicated stream in Fig. 2 is shown in Table 8.

In an AD cycle, there are two pairs of adsorper beds, containing the packed adsorbent (silica gel) in a tube-fin heat exchanger, and regulating the flow of heating and cooling fluids being supplied *via* heating, cooling and chilled water circuits are essential elements of the AD cycle and whereas AD cycle was validated against experimental work as shown in Table 5 [11] and the model conditions is shown in Table 6. The comparison of SDWP between simulated and experimented data is implemented on the 2-bed AD cycle operating over a half-cycle period at different hot water inlet temperatures.

3. Results and discussion

3.1. Numerical model of combined RO-AD system

Hybridisation of brackish water reverse osmosis (BWRO) desalination technology and the adsorption cycle (AD) considered in this work as a means of producing large quantities of water for irrigation and high quality water for domestic use. Fig. 3 shows a schematic diagram of the combined RO-AD system with a recovery device (pressure exchanger). The RO process and the AD cycle are represented as a numerical model to produce fresh water for drinking, irrigation and cooling.

The RO-AD combination can simultaneously produce a cooling effect which can be exploited for process cooling or air conditioning while retrofitting the existing RO plant to improve its specific energy consumption. A pressure exchanger (PX) and AD are combined to recover the reject from RO, resulting in reduction in power consumption. The temperature and feed salinity may negatively effect on RO production however, with the AD cycle producing $> 6\,m^3$/tonne s.g of drinking water (< 10 ppm) at 85 °C, additionally the AD evaporator is

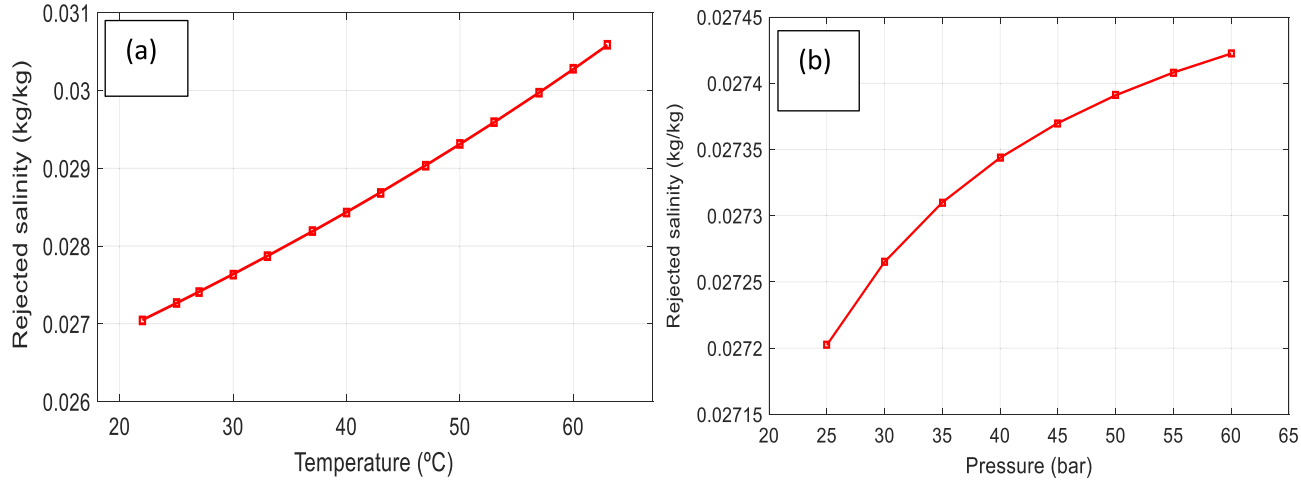

Fig. 5. Rejected salinity as a function of temperature (a) and pressure (b).

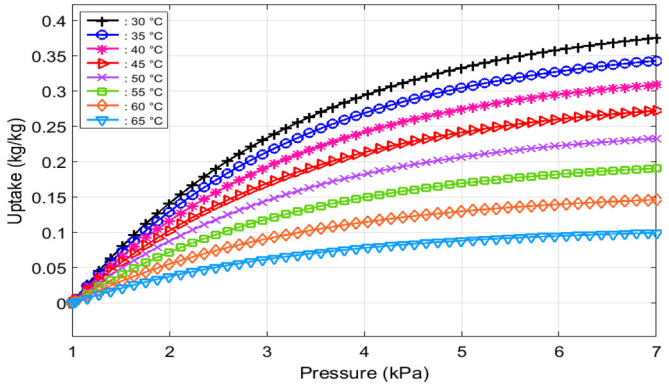

Fig. 8. Uptake of Silica gel at different temperatures at adsorption process.

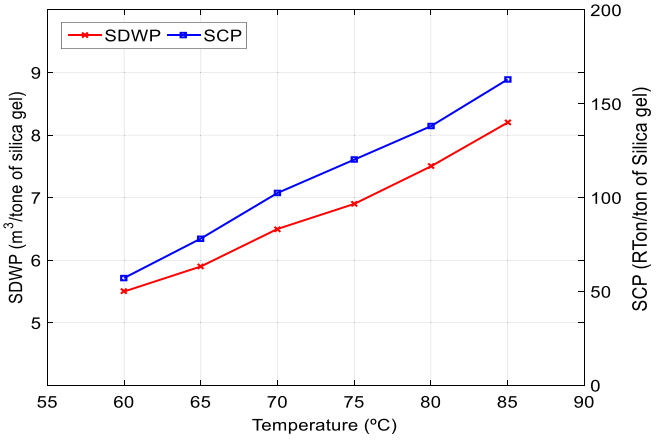

Fig. 9. Effect of bed temperature on SDWP and SCP.

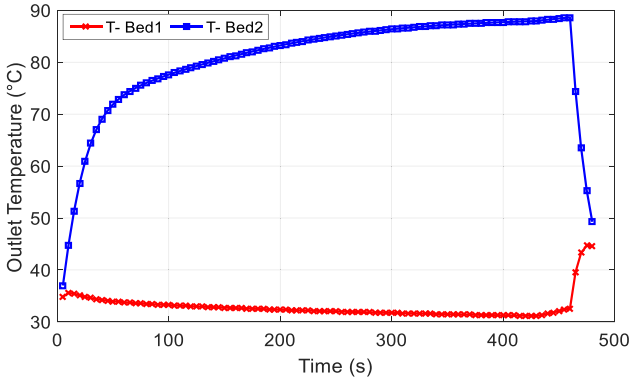

Fig. 10. Outlet temperature profiles of beds for silica gel-water.

not much effected by salinity. The proposed plant could produce 24,000 m^3/day water for irrigation, salinity < 1600 ppm and 6.3 m^3/tonne of silica gel per day for drinking with < 10 ppm as well as cooling 75 RTon/tonne silica gel for air-conditioning.

Eqs. 1 and 19 have been used to calculate permeate flux and specific daily water production (SDWP) for RO and AD processes respectively, and Eq. 18 used for calculating cooling power. The feed salinity could increase the cost of production as shown in Fig. 4, but it is a slightly less with the PX and the same with AD. High feed concentration led to high feed pressure pump due to the increases of osmotic pressure based on Eq. 6. Also, concentration of brine is a function of temperature, pressure and feed salinity as shown in Fig. 5(a) and (b), therefore, an energy recovery device is required to recover the high pressure and salinity concentration in the brine disposal. While, the rejection coefficient is a

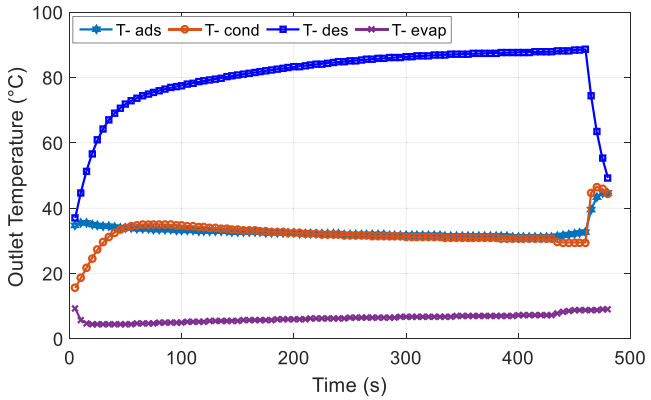

Fig. 11. Outlet temperature of adsorption, desorption, condenser and evaporator.

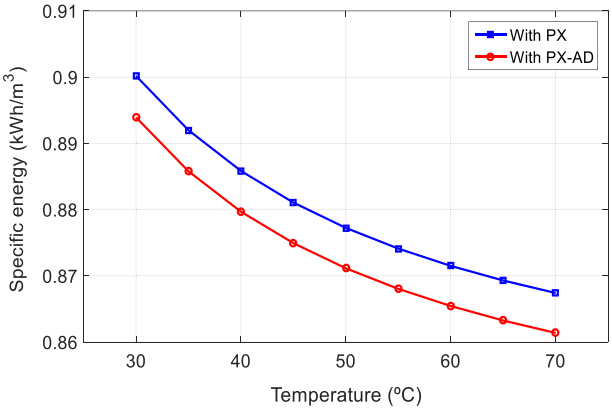

Fig. 12. Specific energy consumption with PX and PX-AD as a function of Bed's temperature.

function of the operating condition, the high pressures increase the salt rejection. Also, salt rejection increases with reducing temperature which means that with higher temperatures, much more TDS is in permeate.

Utilising PX recovery and AD cycle to recover the rejected water from RO, could be a promising solution for RO disposal as the AD evaporator is not effected by high salinity water in the discharge.

For economic analysis, the total combined RO-AD system production is reduced to 2000 m^3/day. Different configurations have been evaluated economically to estimate the production cost including standard RO, RO-ERT, RO-PX and RO-AD system. The AD cycle production was scaled up to be the same as the RO system which is 1000 m^3/day. Fig. 6 illustrates that the cost of the combined RO-AD system is the lowest, 0.44 £/m^3 compares with other RO configurations. The recovery of RO and AD was used in this configurations are 45% and 80% respectively and the overall recovery of the combined RO-AD system is 65%.

In the following analysis and as presented in the schematic in Fig. 3, the evaporator was fed by the rejected water resulting from the RO process, and the desalinated water was collected from the condenser. Rejected water is at high pressure, and as such a recovery device (pressure exchanger) was employed to recycle this energy back into the cycle. Meanwhile, the AD cycle was supplied using the discharge from pressure exchanger. For the purposes of this work, the AD evaporator was supplied with discharged water from the RO.

Employing the mathematical model, the outlet temperature profiles of silica gel – water have been validated against experimental data as shown in Table 5. In addition, the temperature influenced permeate concentration and flow rate (shown in Fig. 7), which are increased due

to the reduction of viscosity, and this could lead to more salinity in the permeate. Temperature was varied from 25 °C to 60 °C to study the RO filtration performance. The isotherm characteristics have been examined of water vapour at temperature and pressures ranging from 30 °C to 65 °C and from 0.001 to 0.07 bar, respectively. Fig. 8 shows the water vapour uptake by silica gel-water at each temperature and the highest capacity of adsorbing is at 30 °C. However, desorption temperature in AD cycle, increases SDWP and SCP when it increases, as shown in Fig. 9 and the AD temperature profiles for two beds is illustrated in Fig. 10. The temperature of bed1 (adsorption) is decreased with the time while the bed2 temperature (desorption) is increased due to the heat water in during the desorption period to realise water vapour.

As presented in the analysis, the outlet temperature of adsorper bed is connected with evaporator during the first half cycle time while the sorption bed is in pre-heating. The evaporator is always connected with one of the beds and it is fed by the rejected from RO unit. Fig. 11 shows the outlet temperature of the two beds, outlet chilled water and condenser cooling water. The cooling is provided from the evaporator due to its low temperature. The conditions of adsorption or desorption of the process is maintained at half-cycle of 480 s, and hot water and cooling water inlet temperatures are 85 °C and 30 °C respectively.

Fig. 12 illustrates that the minimum specific energy for the combined RO-PX-AD plant is 0.8 kWh/m^3 with a capacity of 24,000 m^3/day at RO recovery and temperature are 45% and 25 °C respectively, and 85 °C as heat water in during desorption process. Although, the specific energy consumption is a quite similar between RO-PX scenario and RO-PX-AD scenario, the effect of the energy recovery systems (PX and AD) has been determined. This could lead to a reduction in the cost of production. It has been proven that utilising two recoveries to reuse back the brine is a valuable solution for the RO desalination plants.

Utilising a PX recovery and AD cycle to recover the rejected water from RO, could be a promising solution for RO disposal due to the fact that the AD evaporator is not effected by high salinity water in the rejected. In addition, the analysis shows the effect of temperature in specific power consumption as it is decreased when the temperature increases due to an increase in the permeate flow rate, however the reduction is minimal particularly for the PX. The hybridised RO-AD desalination processes can be considered the optimum solution for rural areas due to the combined production of water for irrigation and drinking as well as cooling for air-conditioning.

4. Conclusions

The performance of hybridised RO-AD model has been investigated numerically and validated. The results show that RO is adversely effected by temperature, however the AD cycle produced 6.3 m^3/day when the hot temperature was 85 °C. The AD evaporator is fed by the rejected water and this lead to reduce the specific power consumption, increase in the production and generating cooling that can be utilised for cooling applications. The feed of salinity influenced the RO production but it is not in AD cycle process. The specific energy of a combined RO-PX-AD plant with a capacity of 24,000 m^3/day is slightly reduced when the temperature increased. Energy recovery device is an important element for minimizing the plant consumption particularly at using of brackish water. It has been proven that utilising of PX recovery and AD cycle to reuse back the disposal brine is a valuable solution for the RO brackish desalination plants.

Acknowledgements

The authors wish to acknowledge the financial support provided by the EPSRC's Thermal Energy Challenge (EP/P005667/1) for the work performed. Data supporting this publication is openly available under an Open Data Commons Open Database License. Additional metadata are available at: http://dx.doi.org/10.17634/152537-1. Please contact Newcastle Research Data Service at rdm@ncl.ac.uk for access instructions.

References

[1] IDA, Worldwide Desalting plant Inventory, Available from, 2014. http://desaldata.com/.
[2] 2030 Water Resources Group, Charting Our Water Future, 5–10. Available from, 2009. http://www.2030waterresourcesgroup.com/water_full/Charting_Our_Water_Future_Final.pdf.
[3] UN Water, Available from: http://www.unwater.org/statistics/statistics-detail/en/c/211204/.
[4] S. Kalogirou, Solar Energy Engineering: Process and Systems, (2009).
[5] C. Li, Y. Goswami, E. Stefanakos, Solar assisted sea water desalination: a review, Renew. Sust. Energ. Rev. 19 (2013) 136–163.
[6] B. Peñate, L. García-Rodríguez, Current trends and future prospects in the design of seawater reverse osmosis desalination technology, Desalination 284 (2012) 1–8.
[7] D.E. Sachit, J.N. Veenstra, Analysis of reverse osmosis membrane performance during desalination of simulated brackish surface waters, J. Membr. Sci. 453 (2014) 136–154.
[8] P.-K. Park, et al., Full-scale simulation of seawater reverse osmosis desalination processes for boron removal: effect of membrane fouling, Water Res. 46 (12) (2012) 3796–3804.
[9] X. Zheng, et al., Seawater desalination in China: retrospect and prospect, Chem. Eng. J. 242 (2014) 404–413.
[10] A. Al-Karaghouli, L.L. Kazmerski, Energy consumption and water production cost of conventional and renewable-energy-powered desalination processes, Renew. Sust. Energ. Rev. 24 (0) (2013) 343–356.
[11] K. Thu, Adsorption Desalination: Theory & Experiments, National University of Singapore, 2010.
[12] J.C. Crittenden, et al., Reverse osmosis, Water Treatment: Principles and Design, Wiley, Hoboken, NJ, 2005, pp. 1456–1468.
[13] Michaels, A.S., High flow membrane. 1971, Google Patents.
[14] R.R. Sharma, S. Chellam, Temperature and concentration effects on electrolyte transport across porous thin-film composite nanofiltration membranes: pore transport mechanisms and energetics of permeation, J. Colloid Interface Sci. 298 (1) (2006) 327–340.
[15] X. Jin, et al., Effects of feed water temperature on separation performance and organic fouling of brackish water RO membranes, Desalination 239 (1–3) (2009) 346–359.
[16] A. Jawor, E.M.V. Hoek, Effects of feed water temperature on inorganic fouling of brackish water RO membranes, Desalination 235 (1–3) (2009) 44–57.
[17] H.T. El-Dessoukya, H.M. Ettouneya, F. Mandani, Performance of Parallel Feed Multiple Effect Evaporation System for Seawater Desalination, (2000).
[18] K.C. Ng, et al., Adsorption Desalination: A Novel Method, (2011).
[19] K.C. Ng, K. Thu, Y.D. Kim, Solar-assisted Adsorption Cycle for the Production of Cooling Effect, (2011).
[20] K.C. Ng, et al., Adsorption desalination: an emerging low-cost thermal desalination method, Desalination 308 (2013) 161–179.
[21] S. Mitra, et al., Simulation study of a two-stage adsorber system, Appl. Therm. Eng. 72 (2) (2014) 283–288.
[22] K. Thu, et al., A synergetic hybridization of adsorption cycle with the multi-effect distillation (MED), Appl. Therm. Eng. 62 (1) (2014) 245–255.
[23] S. Mitra, et al., Solar driven adsorption desalination system, Energy Procedia 49 (2014) 2261–2269.
[24] K. Ng, et al., Adsorption Desalination: A Novel Method, in: L. Wang, et al. (Ed.), Membrane and Desalination Technologies, Humana Press, 2011, pp. 391–431.
[25] S. Mitra, et al., Modeling study of two-stage, multi-bed air cooled silica gel + water adsorption cooling cum desalination system, Appl. Therm. Eng. 114 (Supplement C) (2017) 704–712.
[26] K. Thu, et al., Performance investigation on a 4-bed adsorption desalination cycle with internal heat recovery scheme, Desalination 402 (Supplement C) (2017) 88–96.
[27] K. Thu, et al., Modeling and simulation of mass recovery process in adsorption system for cooling and desalination, Energy Procedia 105 (Supplement C) (2017) 2004–2009.
[28] K.C. Ng, et al., Solar-assisted dual-effect adsorption cycle for the production of cooling effect and potable water, Int. J. Low Carbon Technol. 4 (2) (2009) 61–67.
[29] K.C. Ng, et al., Study on a waste heat-driven adsorption cooling cum desalination cycle, Int. J. Refrig. 35 (3) (2012) 685–693.
[30] X. Wang, K.C. Ng, Experimental investigation of an adsorption desalination plant using low-temperature waste heat, Appl. Therm. Eng. 25 (17–18) (2005) 2780–2789.
[31] A.M. Helal, et al., Optimal design of hybrid RO/MSF desalination plants part II: results and discussion, Desalination 160 (1) (2004) 13–27.
[32] K.C. Ng, et al., Recent developments in thermally-driven seawater desalination: energy efficiency improvement by hybridization of the MED and AD cycles, Desalination 356 (2015) 255–270.
[33] S. Mitra, et al., Performance evaluation of a two-stage silica gel + water adsorption based cooling-cum-desalination system, Int. J. Refrig. 58 (Supplement C) (2015) 186–198.
[34] K. Thu, et al., Performance investigation of a waste heat-driven 3-bed 2-evaporator adsorption cycle for cooling and desalination, Int. J. Heat Mass Transf. 101 (Supplement C) (2016) 1111–1122.

[35] K. Thu, et al., Performance investigation of an advanced multi-effect adsorption desalination (MEAD) cycle, Appl. Energy 159 (Supplement C) (2015) 469–477.
[36] B.A. Qureshi, S.M. Zubair, Energy-exergy analysis of seawater reverse osmosis plants, Desalination 385 (2016) 138–147.
[37] A. Al-Zahrani, et al., Thermodynamic analysis of a reverse osmosis desalination unit with energy recovery system, Procedia Eng. 33 (2012) 404–414.
[38] W. Zhou, L. Song, T.K. Guan, A numerical study on concentration polarization and system performance of spiral wound RO membrane modules, J. Membr. Sci. 271 (1–2) (2006) 38–46.
[39] M. Sarai Atab, A.J. Smallbone, A.P. Roskilly, An operational and economic study of a reverse osmosis desalination system for potable water and land irrigation, Desalination 397 (2016) 174–184.
[40] J.G. Wijmans, R.W. Baker, The solution-diffusion model: a review, J. Membr. Sci. 107 (1–2) (1995) 1–21.
[41] S. Lee, R.M. Lueptow, Membrane Rejection of Nitrogen Compounds, (2001).
[42] M. Cheryan, Ultrafiltration and Microfiltration Handbook, CRC press, 1998.
[43] R. Rautenbach, R. Albrecht, Membrane Processes, John Wiley and Sons Ltd, West Germany, 1981.
[44] S.A. Avlonitis, M. Pappas, K. Moutesidis, A unified model for the detailed investigation of membrane modules and RO plants performance, Desalination 203 (1–3) (2007) 218–228.
[45] R.W. Baker, Membrane Technology and Applications, John Wiley & Sons, Ltd., Chichester, 2004.
[46] B. Shi, et al., CPO-27(Ni) metal–organic framework based adsorption system for automotive air conditioning, Appl. Therm. Eng. 106 (2016) 325–333.
[47] S.K. Henninger, et al., Evaluation of methanol adsorption on activated carbons for thermally driven chillers part I: thermophysical characterisation, Int. J. Refrig. 35 (3) (2012) 543–553.
[48] P.G. Youssef, R.K. Al-Dadah, S.M. Mahmoud, Comparative analysis of desalination technologies, Energy Procedia 61 (2014) 2604–2607.
[49] M. Suzuki, Adsorption Engineering, Elsevier, 1990.
[50] D.M. Ruthven, Principles of Adsorption and Adsorption Processes, John Wiley & Sons, 1984.
[51] K. Chihara, M. Suzuki, Air drying by pressure swing adsorption, J. Chem. Eng. Jpn 16 (4) (1983) 293–299.